International Journal of Pharmaceutics 429 (2012) 46–57

Contents lists available at SciVerse ScienceDirect

International Journal of Pharmaceutics

journal homepage: www.elsevier.com/locate/ijpharm

Effect of process variables on morphology and aerodynamic properties of voriconazole formulations produced by thin film freezing

Nicole A. Beinborn*, Hélène L. Lirola, Robert O. Williams III*

Division of Pharmaceutics, College of Pharmacy, The University of Texas at Austin, TX, United States

ARTICLE INFO

Article history:
Received 15 August 2011
Received in revised form 1 March 2012
Accepted 6 March 2012
Available online 13 March 2012

Keywords:
Poorly water-soluble drug
Crystalline
Amorphous
Dry powder inhalation
Ultra-rapid freezing, nanotechnology

ABSTRACT

The particle engineering process, thin film freezing (TFF), was used to produce particulate voriconazole (VRC) formulations with enhanced properties. The effect of various processing parameters on the solid state properties and aerodynamic performance of the TFF-processed powders was investigated in order to evaluate the suitability of these formulations for dry powder inhalation and to optimize the aerodynamic properties. Thin film freezing of VRC solution without stabilizing excipients resulted in microstructured, crystalline low density aggregate particles with specific surface areas of approximately 10 m^2/g. Thin film freezing of VRC–PVP solutions produced nanostructured, amorphous low density aggregate particles with specific surface areas ranging from 15 to 180 m^2/g, depending on the solvent system composition, polymer grade, and drug to polymer ratio utilized. VRC formulations manufactured with 1,4-dioxane, with and without PVP K12, resulted in the lowest specific surface areas but displayed the best aerodynamic properties. Using a Handihaler® dry powder inhaler (DPI), microstructured crystalline TFF–VRC and nanostructured amorphous TFF–VRC–PVP K12 (1:2) displayed total emitted fractions of 80.6% and 96.5%, fine particle fractions of 43.1% and 42.4%, and mass median aerodynamic diameters of 3.5 and 4.5 μm, respectively.

1. Introduction

A significant number of the new chemical entities developed using high throughput screening techniques exhibit increased molecular weight and lipophilicity but poor aqueous solubility (Lipinski, 2000). Numerous strategies and processes have been reported to create pharmaceutical formulations with enhanced properties to facilitate dissolution of these poorly water soluble drugs, including particle size reduction by milling, homogenization, antisolvent precipitation, and formation of amorphous solid dispersions by spray drying, hot melt extrusion, supercritical fluid technologies, and cryogenic methods (Leuner and Dressman, 2000; Zhang et al., 2011). In addition, particle engineering for pulmonary drug delivery has gained interest in recent years in response to the need for tailor-made drug particles with enhanced properties capable of more efficient delivery to the lungs (Chow et al., 2007; Zhang et al., 2011). There are several advantages for engineered particles in pulmonary drug delivery: (1) nanoparticles and large porous particles have been shown to improve the fine particle fraction emitted from dry powder inhalers compared to micronized particles thus increasing the amount of drug that deposits in the lung (Bhavna Ahmad et al., 2009; Edwards et al., 1997), (2) particles with diameters less than 100 nm or more than 10 μm have shown evidence of greatly reduced macrophage clearance, enabling the possibility for sustained lung concentrations and increased time for dissolution (Yang et al., 2008a; Zhang et al., 2011), (3) the higher energy state of amorphous polymorphs and the increased surface area of nanoparticles may enhance rate and extent of drug dissolution in the lung lining fluid (Yang et al., 2008b). The particle engineering process, thin film freezing (TFF), has been shown to produce low density pharmaceutical powders composed of porous nanostructured aggregate particles. When stabilizing excipients with high glass transition temperatures, such as PVP or HPMC, are included in the formulation, the pharmaceutical powders can be rendered amorphous (Overhoff et al., 2009). These low density TFF-processed powders have also been reported to be highly respirable when aerosolized with a commercially marketed dry powder inhaler (DPI) (Johnston et al., 2010).

Attention has begun to focus on the pulmonary delivery of antifungal agents as inhalation of the fungal spores is often the first step in the pathogenesis of invasive fungal infections in the lungs (Doffman et al., 2005; Xie et al., 2008). Voriconazole (VRC) is a second generation triazole antifungal agent. Compared to

* Corresponding authors. Current address: The University of Texas at Austin, College of Pharmacy, 1 University Station, Mail Stop A1920, Austin, TX 78712, USA. Tel.: +1 512 471 4681; fax: +1 512 471 7474.
E-mail addresses: nicolebeinborn@gmail.com (N.A. Beinborn), williro@mail.utexas.edu (R.O. Williams III).

0378-5173/$ – see front matter © 2012 Elsevier B.V. All rights reserved.
doi:10.1016/j.ijpharm.2012.03.010

fluconazole, a first generation triazole, VRC has increased potency and a broader spectrum of activity but lower aqueous solubility (Roffey et al., 2003). VRC is considered a BCS Class II molecule, with high permeability and low solubility in vivo, although the solubility is just below the boundary for BCS I classification (high permeability, high solubility) (FDA, 2000). The water solubility is approximately 0.7 mg/mL, but increases to more than 3 mg/mL in acidic conditions (Buchanan et al., 2007; Roffey et al., 2003). Nonetheless, complexation with sulfobutyl ether-β-cyclodextrin is required to solubilize VRC for intravenous administration (Pfizer, 2011).

Previously, our research group has investigated and modeled the freezing rate and thin film geometry of *tert*-butanol and acetonitrile during the thin film freezing process. Despite possessing considerably different solvent properties, and consequently, resulting in very different freezing rates and thin film thickness and diameters upon impingement, these solvents did not significantly affect the physicochemical properties of amorphous solid dispersions containing danazol and PVP produced by TFF (Overhoff et al., 2007). However, an in-depth investigation of the freezing rate and thin film geometry has not been conducted with 1,4-dioxane and 1,4-dioxane:water cosolvent systems. Furthermore, few studies have reported generation of amorphous solid dispersions containing voriconazole or particulate voriconazole formulations for inhalation (Sinha and Mukherjee, 2012; Sundaram et al., 2008).

The objectives of this study are to use thin film freezing to produce particulate VRC formulations with enhanced properties that are suitable for dry powder inhalation and to investigate how process parameters, including the effect of stabilizing excipients, drug to excipient ratio, solvent system composition, and percentage of dissolved solids in the liquid feed solution, affect the morphology and aerodynamic properties of the resulting formulations. We hypothesize that: (1) thin film freezing of organic or aqueous-organic cosolvent solutions containing VRC will result in low density, brittle matrix particles, which can be sheared in situ during aerosolization from a passive inhalation dry powder inhaler to produce highly respirable particles, (2) formulation of VRC with high glass transition temperature excipients using TFF will produce amorphous solid dispersions with high surface areas, (3) solvent properties will affect droplet spreading during the TFF process which will affect the physicochemical properties of the resulting VRC formulations, and (4) solid state properties will influence aerodynamic performance of TFF-processed powders containing VRC.

2. Materials and methods

2.1. Materials

The following materials were purchased: voriconazole (Tecoland Corporation, Edison, NJ); ACS grade 1,4-dioxane, HPLC grade methanol, and lactose monohydrate (Fisher Scientific, Pittsburgh, PA); polyvinylpyrrolidone K30 (Povidone K-30, USP) and polysorbate 80 (Spectrum, Gardena, CA); and ethanol (Decon Labs, King of Prussia, PA). The following materials were generously donated: polyvinylpyrrolidone K12 (Plasdone® K-12, ISP Technologies, Wayne, NJ) and hydroxypropyl methylcellulose (HPMC) K3 (Methocel™ K3, Dow Chemical Company, Midland, MI).

2.2. Solubility of VRC in 1,4-dioxane

An excess of VRC was weighed into a scintillation vial containing 1,4-dioxane at 20 °C and the vial was mixed by vortexing. The suspension was allowed to settle before the supernatant was withdrawn and passed through a 0.2 μm PTFE filter. The solution was diluted with mobile phase and injected into the HPLC for quantitative analysis.

2.3. Formulation preparation

Thin film freezing technology, as described previously (Overhoff et al., 2007), was used to produce voriconazole powders that may be suitable for dry powder inhalation. TFF process parameters, including the effect of stabilizing excipient, drug to excipient ratio, solvent system composition, and the percentage of dissolved solids in the liquid feed solution, were varied. Briefly, VRC and excipients were dissolved in 1,4-dioxane or deionized water, depending on solute solubility. The organic and aqueous phases were combined slowly with continuous mixing to form cosolvent systems. The solutions were frozen drop-wise onto a rotating cryogenic, steel surface (precooled with liquid nitrogen to approximately −40 °C) to produce thin films, removed from the steel surface by a scraper and maintained in the frozen state in liquid nitrogen. Solvents were sublimated by lyophilization using a Virtis Advantage tray lyophilizer to obtain dry powders. Lyophilization was performed over 48 h at pressures less than 200 mTorr while the shelf temperature was gradually ramped from −40 °C to 25 °C. The dried powders were removed from the lyophilizer after nitrogen gas was bled into the lyophilization chamber to equilibrate to atmospheric pressure, then stored in transparent vacuum desiccators at room temperature. Table 1 summarizes the TFF formulations produced in this study. Most of the formulations were prepared at least 3 times on different days to confirm reproducibility of the physicochemical properties.

2.4. Scanning electron microscopy (SEM)

SEM was used to examine the surface morphology and to qualitatively estimate the primary particle size of the TFF powder aggregates. Samples were loaded onto double sided carbon tape and sputter coated with a 60/40 Pd/Au target for 2 min. SEM images were captured using a Leo 1530 scanning electron microscope or an FEI Quanta 650 scanning electron microscope under high vacuum mode with an operating voltage of 3–10 kV.

2.5. Differential scanning calorimetry (DSC)

Thermal analysis of VRC and physical mixtures containing VRC was conducted using a TA Instruments Model 2920 DSC coupled with TA Universal Analysis 2000 Software (New Castle, DE). Prior to testing, physical mixtures of VRC and excipient were prepared in a mortar and pestle by accurately dispensing each component and mixing for approximately 2 min. Samples were weighed to 10–15 mg in an aluminum pan and crimped with an aluminum lid (PerkinElmer, Waltham, MA), then heated at a ramp rate of 10 °C/min under nitrogen purge at a flow rate of 40 mL/min.

Amorphous pure VRC was prepared by quench cooling in liquid nitrogen. Accurately weighed crystalline VRC (as received from the supplier) was heated in a sealed aluminum pan to 200 °C to ensure complete melting. The sample was then quench cooled externally from the DSC instrument by placing the pan in liquid nitrogen. Modulated DSC was conducted by placing the pan back into a precooled sample chamber and the thermogram was recorded using a ramp rate of 10 °C/min with a modulation temperature amplitude of 1 °C and a modulation period of 60 s under nitrogen purge at a flow rate of 40 mL/min. Modulated DSC was also used to measure the glass transition temperatures of the polymers, as well as, the glass transition temperatures and the presence or the absence of the VRC melting endotherm in TFF-processed powders.

Table 1
Summary of VRC formulations produced by TFF.

Sample composition	Drug:excipient ratio	Dissolved solids	Solvent compositions
TFF–VRC	No excipient	0.1% (w/v)	50:50 (v/v) 1,4-dioxane:water
		1% (w/v)	1,4-Dioxane 50:50 (v/v) 1,4-dioxane:water
		10% (w/v)	1,4-Dioxane
TFF–VRC–PVP K12	1:2	1% (w/v)	1,4-Dioxane 50:50 (v/v) 1,4-dioxane:water 50:50 (v/v) 1,4-dioxane:water
TFF–VRC–PVP K30	1:2	0.1% (w/v)	50:50 (v/v) 1,4-dioxane:water
		1% (w/v)	1,4-Dioxane 50:50 (v/v) 1,4-dioxane:water 20:80 (v/v) 1,4-dioxane:water
		10% (w/v)	50:50 (v/v) 1,4-dioxane:water
	1:3	1% (w/v)	50:50 (v/v) 1,4-dioxane:water
TFF–VRC–LAC	1:2	1% (w/v)	50:50 (v/v) 1,4-dioxane:water
TFF–VRC–LAC–PVP K30	1:1:1	1% (w/v)	50:50 (v/v) 1,4-dioxane:water
TFF–VRC–HPMC K3	1:3	1% (w/v)	50:50 (v/v) 1,4-dioxane:water

The melting point for VRC is reported to be 128–134 °C (Herbrecht, 2004).

2.6. Powder X-ray diffraction (XRD)

A Philips 1710 X-ray diffractometer (Cu Kα1 radiation, λ = 1.54059 Å, 40 kV, 40 mA) was used to assess crystallinity in VRC formulations. The pharmaceutical powders were loaded into channeled stages and the diffraction profile was measured from 5° to 40° using a 2Θ step size of 0.05° and a dwell time of 2 s.

2.7. Brunauer–Emmett–Teller (BET) specific surface area (SSA) analysis and powder density

Monosorb MS-21 rapid surface area analyzer was used to measure SSA of the pharmaceutical powders by single point measurement at $P/P_0 = 0.294$. Samples were degassed for at least 2 h under nitrogen purge at 20 psi and 30 °C. The Monosorb utilizes a modified BET equation for extremely rapid, single-point determinations of surface area. 30% nitrogen in helium was used as the adsorbate gas.

Powders were gently poured from a beaker into a 50 mL graduated cylinder. The mass and volume were recorded to calculate the bulk density of the material.

2.8. Aerodynamic particle size analysis

A Next Generation Pharmaceutical Impactor (NGI) (MSP Corp., Shoreview, MN) was used to determine aerodynamic properties of the dried TFF-processed powders. Since coarse lactose particles are not included in the TFF-processed powders for dry powder inhalation, the pre-separator was not used. The powders were filled into size 3 HPMC capsules and aerosolized using a Handihaler® DPI. The DPI was attached to the induction port of the NGI by a molded silicone adapter and actuated over 4 s at a flow rate of 60 L/min. NGI collection surfaces were coated with 1% (v/v) polysorbate 80 in ethanol to prevent particle bounce, fracture, and reentrainment, which would result in a biased skew toward smaller aerodynamic diameter (Mitchell, 2003; USP, 2010a). After aerosolization, all collection surfaces were rinsed with known volumes of mobile phase. The solutions were passed through a 0.2 μm PTFE filter and analyzed by HPLC for VRC content.

Emitted fraction (EF) was calculated as the percentage of drug emitted from the DPI with respect to the total assayed dose recovered from the DPI, silicone adapter, induction port, and NGI collection plates. Mass median aerodynamic diameter (MMAD) and geometric standard deviation (GSD) were calculated based on the dose deposited on stages 1 through 7 and the micro-orifice collector (MOC), as defined in the USP 32-NF 27 General Chapter 601: Aerosols, Nasal sprays, Metered-dose inhalers, and Dry powder inhalers. Fine particle fraction (FPF) was determined from the amount of VRC collected from stages 2 through MOC, which represents the percentage of emitted particles with an MMAD of 4.5 μm or less. FPF estimates the fraction of particles expected to deposit deep within the lungs.

2.9. Chromatographic analysis

VRC content was quantified using a Dionex high performance liquid chromatography (HPLC) system equipped with a reversed-phase Jupiter® C18 column (150 mm × 4.6 mm, 5 μm, 300 Å) with a Universal security guard (Widepore C18) column (Phenomenex, Torrance, CA). The method was adapted from a previously reported method (Pascual et al., 2007). The mobile phase was 50/50 (v/v) methanol/water. VRC eluted at approximately 8 min at 35 °C with a flow rate of 1 mL/min and a detection wavelength of 254 nm. The limit of detection, 3 times the signal to noise ratio (S/N), was 20 ng/mL and the limit of quantification, 10 times S/N, was 75 ng/mL. Linearity test solutions were prepared from a VRC stock solution at eight concentration levels. The peak area versus concentration data was treated by least squares linear regression analysis. The method exhibited linearity greater than 0.99 up to a concentration of 30 μg/mL.

2.10. Statistical analysis

One-way ANOVA, with Tukey–Kramer post hoc test where necessary, using JMP® 8 (SAS Institute, Inc., Cary, NC) was used to statistically compare formulations. Results with *p*-values less than 0.05 were considered statistically significant.

3. Results

3.1. Preformulation studies

1,4-Dioxane was found to be an ideal solvent for VRC and the TFF process. It is miscible with water, has a melting point of 12 °C, density of 1.03 g/mL, and viscosity of 1.54 cP at 20 °C (FisherScientific, 2009). The solubility of VRC in 1,4-dioxane was found to be about 240 mg/mL at 20 °C. One drawback is that 1,4-dioxane is a Class

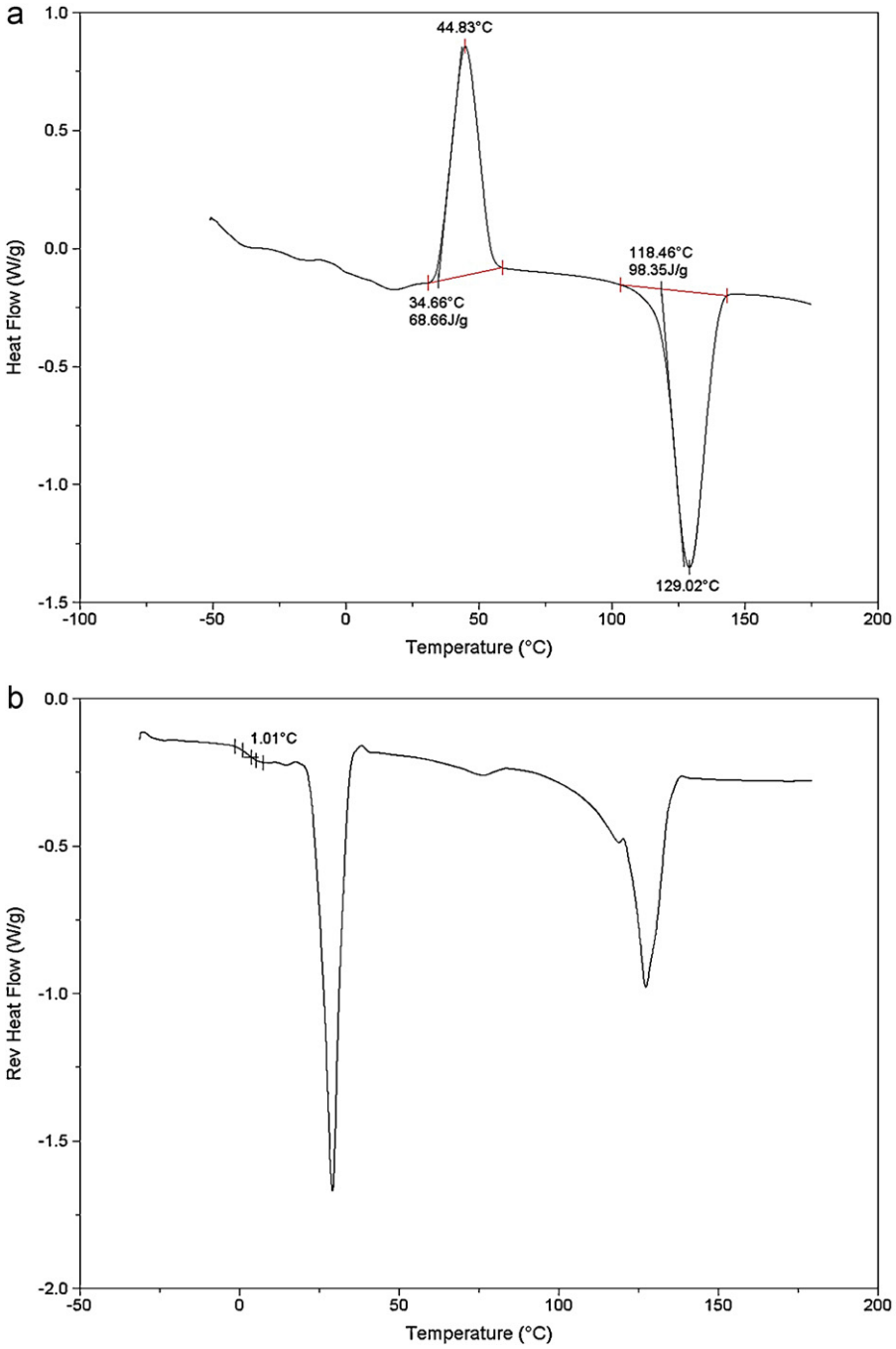

Fig. 1. (a) modulated DSC heat flow thermogram of quench cooled VRC and (b) modulated DSC reversed heat flow thermogram of quench cooled VRC.

2 solvent, with inherent toxicities, and is therefore limited to a residual solvent concentration of 380 ppm (USP, 2010b). Residual 1,4-dioxane concentrations were not measured in this study.

Modulated differential scanning calorimetry was employed to determine the glass transition temperature of pure VRC. Fig. 1a shows the modulated DSC heat flow thermogram which indicates a recrystallization event of VRC at about 45 °C and the melting endotherm at 129 °C. The recrystallization event confirms the production of amorphous VRC by the quench cooling process; and therefore, the modulated DSC reversed heat flow thermogram (Fig. 1b) shows that the glass transition of VRC is approximately 1 °C. The glass transition temperatures of PVP K12 and PVP K30 were found to be approximately 127 °C and 164 °C, respectively.

Physical mixtures tested using DSC were examined for the presence of melting and drug dissolution events associated with VRC (Fig. 2). Crystalline VRC has a melting endotherm observed at 131 °C, with a heat of fusion of 121 J/g. The physical mixtures comprising VRC and PVP K12 contain 33%, 50% and 75% VRC. The expected heats of fusion for VRC in the physical mixtures are calculated based on weight fraction, i.e. the expected heat of fusion of VRC in a 1 to 1 mixture would be approximately 60.5 J/g. Noting that the heats of fusion for VRC in the physical mixtures are 16.5, 35.8, and 78.8 J/g, respectively, these values correspond to approximately 41%, 59%, and 87% recovery (ratio of actual heat of fusion to expected heat of fusion) of crystalline VRC from the tests, indicating some dissolution of VRC into PVP upon heating (Dinunzio et al., 2010; Forster et al., 2001). Additionally, a slight melting point depression of VRC is observed in the presence of PVP. The physical mixtures comprising VRC and HPMC K3 contain 25%, 50% and 75% VRC. Noting that the heats of fusion of the physical mixtures

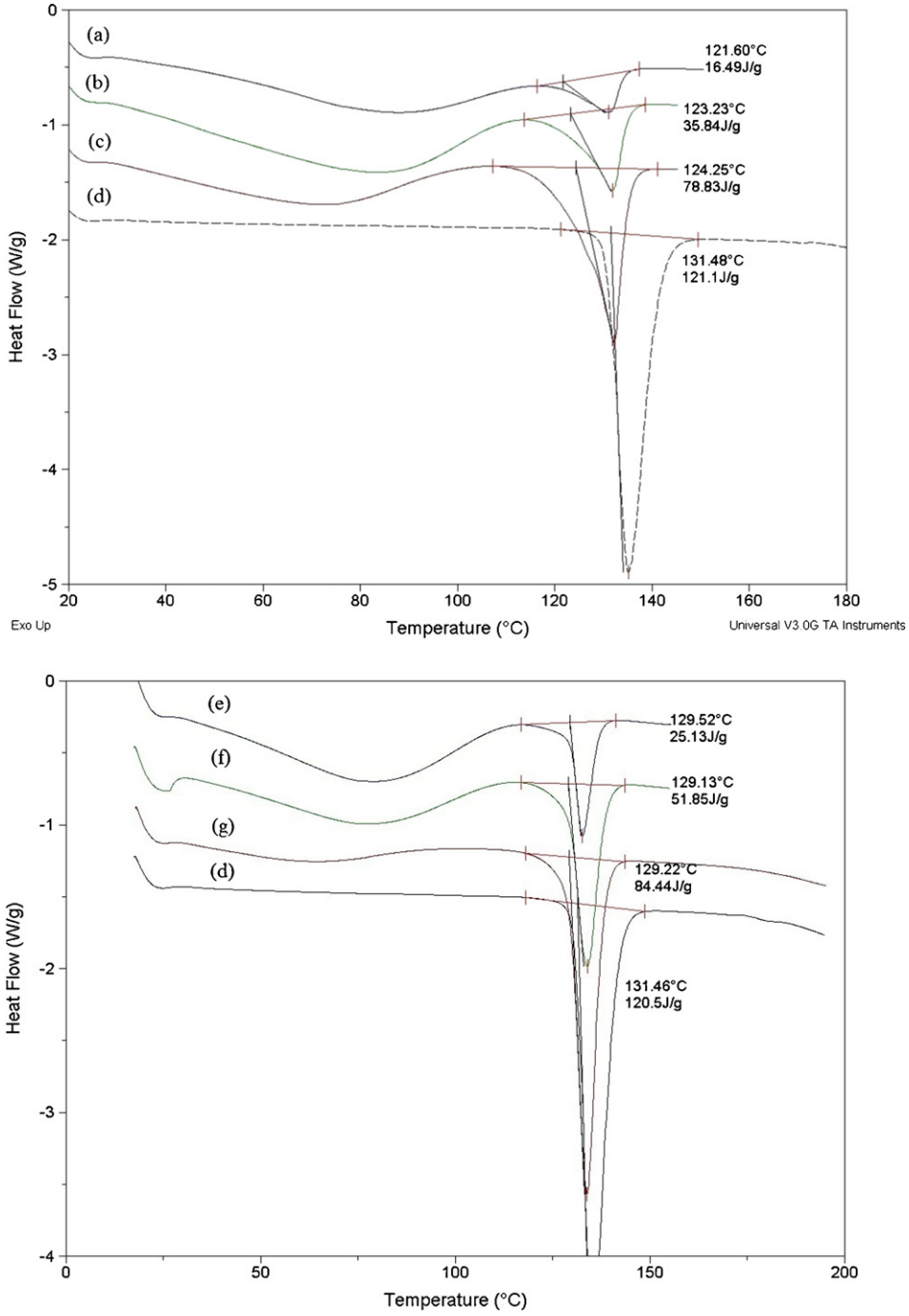

Fig. 2. Excipient screening by DSC. (a) 1 to 2 physical mixture of VRC to PVP K12; (b) 1 to 1 physical mixture of VRC to PVP K12; (c) 3 to 1 physical mixture of VRC to PVP K12; (d) crystalline VRC (as received from supplier); (e) 1 to 3 physical mixture of VRC to HPMC K3; (f) 1 to 1 physical mixture of VRC to HPMC K3; and (g) 3 to 1 physical mixture of VRC to HPMC K3.

are 25.1, 51.8, and 84.4 J/g, respectively, these values correspond to approximately 83%, 86%, and 93% recovery of crystalline VRC from the tests, indicating very little dissolution of VRC into HPMC upon heating. Furthermore, there is no melting point depression of VRC in the presence of HPMC.

3.2. Physicochemical properties of TFF formulations

SEM images indicate that thin film freezing of VRC solution without stabilizing excipients results in large aggregate particles with microstructured primary particles (Fig. 3) and thin film freezing of VRC–PVP solutions result in large aggregate particles with nanostructured primary particles with a size of approximately 100 nm (Fig. 4). The powder X-ray diffraction patterns and the modulated DSC thermograms of the TFF-processed powders are shown in Figs. 5 and 6, respectively. All TFF–VRC formulations exhibited crystalline morphology. Polymeric stabilization was required to produce amorphous solid dispersions containing VRC by the TFF particle engineering process. Lactose monohydrate (alone or in combination with PVP) was not a sufficient stabilizing excipient for amorphous voriconazole at the desired drug loading, despite a relatively high glass transition temperature of about 100 °C (Gabbott et al., 2003). HPMC K3 was able to stabilize VRC in the amorphous state using a 1 to 3 drug to polymer ratio, as indicated by XRD, but

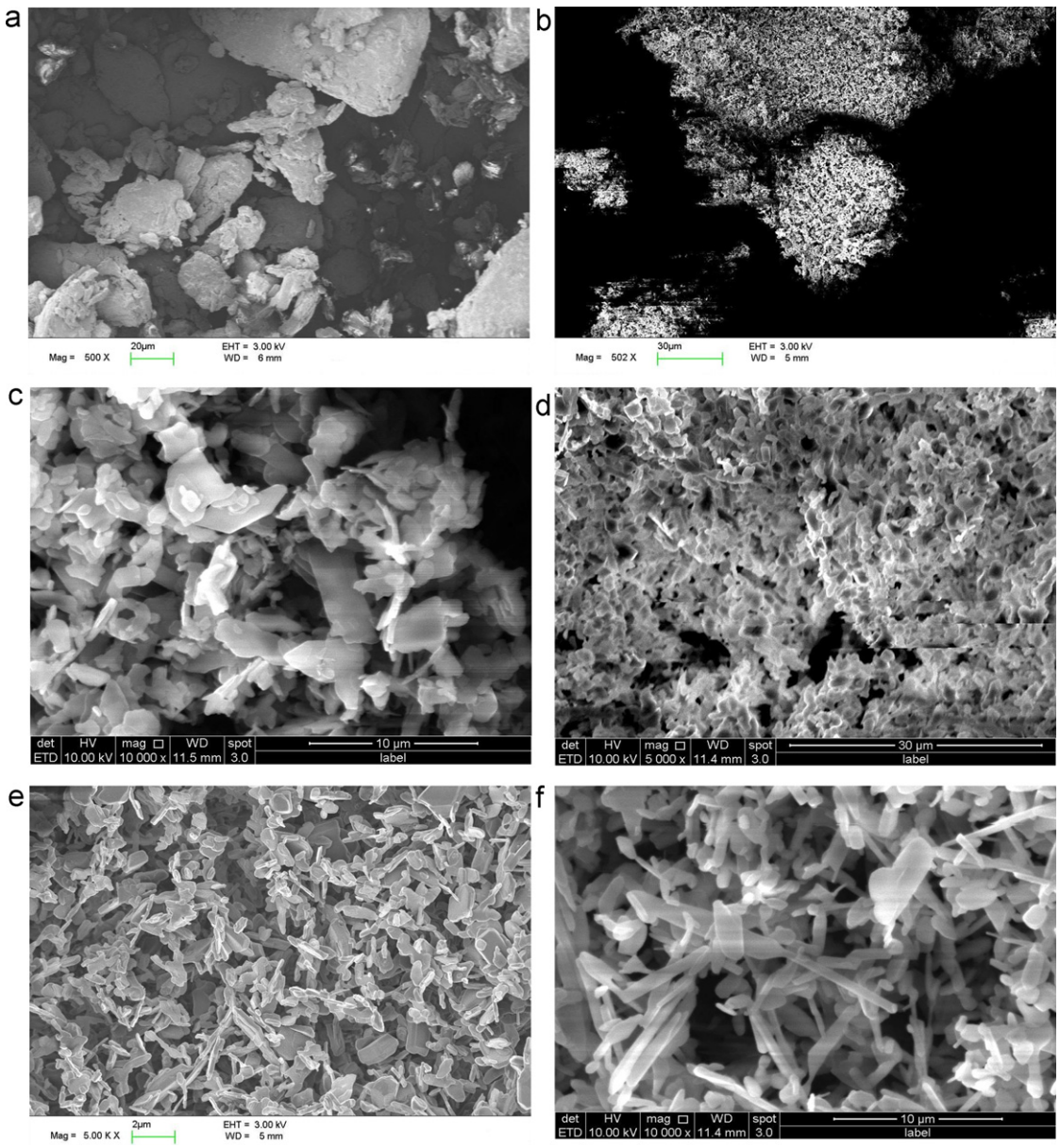

Fig. 3. SEM images of crystalline VRC (as received from supplier) and microstructured crystalline TFF–VRC. (a) Crystalline VRC (as received from supplier); (b) TFF–VRC aggregate particle at 500X magnification; primary particle structure of TFF–VRC powders made with various processing parameters: (c) TFF–VRC prepared by 0.1% (w/v) in 50:50 1,4-dioxane:water at 10,000× magnification; (d) TFF–VRC prepared by 10% (w/v) in 1,4-dioxane at 5000× magnification; (e) TFF–VRC prepared by 1% (w/v) in 50:50 1,4-dioxane:water at 5000× magnification; and (f) TFF–VRC prepared by 1% (w/v) in 1,4-dioxane at 10,000× magnification.

the powder was too sticky to be suitable for dry powder inhalation. The SSA and bulk densities of the TFF formulations are reported in Table 2.

The solvent system composition and the dissolved solids content in the liquid feed solution had a considerable effect on the macroscopic appearance of the TFF-processed powders. As seen in Fig. 7, TFF-processed powders (both crystalline and amorphous) manufactured using 1% (w/v) dissolved solids in 100% 1,4-dioxane resulted in powder with significant agglomeration; whereas, TFF-processed powders made from 0.1% (w/v) or 1% (w/v) dissolved solids in 50:50 (v/v) 1,4-dioxane:water yielded a fine, fluffy powder with no agglomeration. Furthermore, TFF formulations prepared from 1% (w/v) dissolved solids in 20:80 (v/v) 1,4-dioxane:water resulted in material with a flake-like appearance. Similarly, when the dissolved solids content was increased to 10% (w/v), the material was also composed of thin flakes; however, these flakes were not as brittle as the other TFF-processed powders prepared using lower dissolved solids content.

3.3. *In vitro aerosol performance of TFF formulations containing VRC with and without PVP*

Aerodynamic particle size distribution of the TFF-processed powders was assessed using a Handihaler® DPI device and an NGI apparatus. The Handihaler®, a single dose capsule-based DPI, was chosen for aerosolization of the low density aggregate particles because it was anticipated that this device would provide the shearing force necessary to break up the large aggregates into respirable particles in situ as the powder is aerosolized by inhalation out from the punctured capsule. The aerodynamic properties are shown in Table 3. In some of the test runs, more than 50% of the particles deposited on stage 1; consequently, MMAD and GSD

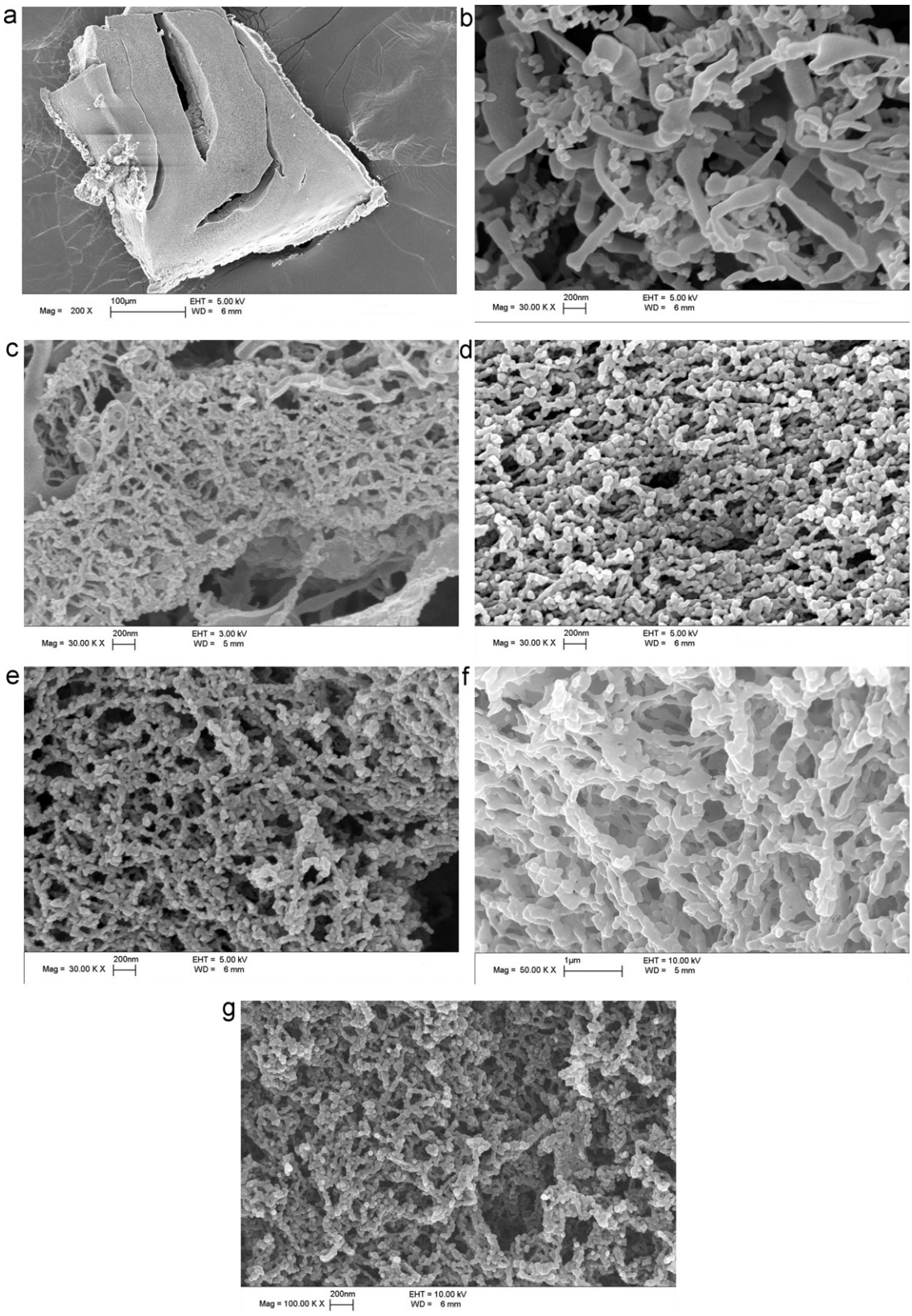

Fig. 4. SEM images of nanostructured solid dispersions produced by TFF. (a) TFF–VRC–PVP aggregate particle; primary particle structure of TFF–VRC–PVP powders made with various processing parameters: (b) TFF–VRC–PVP K12 (1:2) prepared by 1% (w/v) in 1,4-dioxane; (c) TFF–VRC–PVP K30 (1:2) prepared by 1% (w/v) in 1,4-dioxane; (d) TFF–VRC–PVP K12 (1:2) prepared by 1% (w/v) in 50:50 1,4-dioxane: water; (e) TFF–VRC–PVP K30 (1:2) prepared by 1% (w/v) in 50:50 1,4-dioxane:water; (f) TFF–VRC–PVP K12 (1:2) prepared by 1% (w/v) in 20:80 1,4-dioxane:water; and (g) TFF–VRC–PVP K30 (1:2) prepared by 1% (w/v) in 20:80 1,4-dioxane:water.

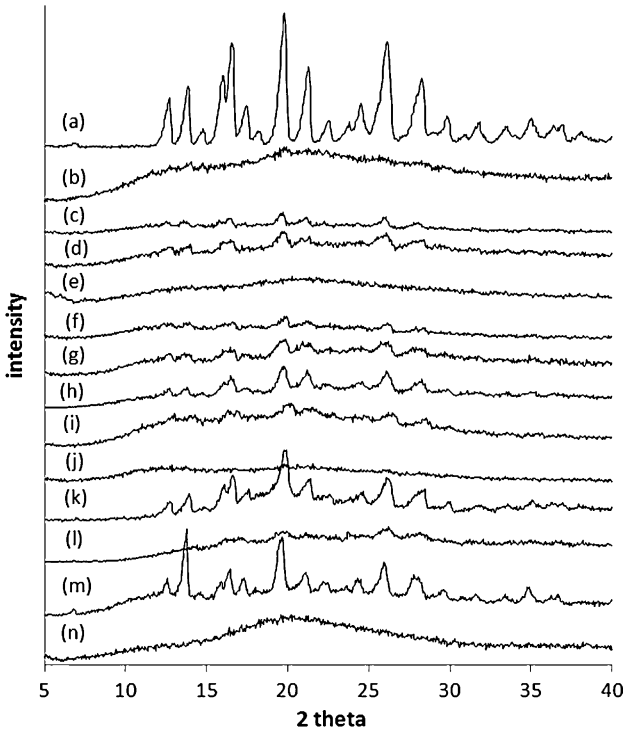

Fig. 5. Powder X-ray diffraction patterns. (a) TFF–VRC; (b) TFF–VRC–PVP K12 (1:2) prepared by 1% (w/v) in 1,4-dioxane; (c) TFF–VRC–PVP K12 (1:2) prepared by 1% (w/v) in 50:50 1,4-dioxane:water; (d) TFF–VRC–PVP K12 (1:2) prepared by 1% (w/v) in 20:80 1,4-dioxane:water; (e) TFF–VRC–PVP K30 (1:2) prepared by 1% (w/v) in 1,4-dioxane; (f) TFF–VRC–PVP K30 (1:2) prepared by 1% (w/v) in 50:50 1,4-dioxane:water; (g) TFF–VRC–PVP K30 (1:2) prepared by 1% (w/v) in 20:80 1,4-dioxane:water; (h) TFF–VRC–PVP K30 (1:2) prepared by 0.1% (w/v) in 50:50 1,4-dioxane:water; (i) TFF–VRC–PVP K30 (1:2) prepared by 10% (w/v) in 50:50 1,4-dioxane:water; (j) TFF–VRC–PVP K30 (1:3); (k) TFF–VRC–LAC (1:2); (l) TFF–VRC–LAC–PVP K30 (1:1:1); (m) 1 to 2 physical mixture of VRC to PVP; and (n) TFF–VRC–HPMC K3 (1:3).

could not be accurately calculated in these cases. Comparing all of the microstructured crystalline formulations, TFF–VRC prepared from 1% (w/v) in 100% 1,4-dioxane displayed the best aerodynamic properties from the Handihaler® DPI. Likewise, TFF–VRC–PVP K12 (1:2) prepared from 1% (w/v) 100% dioxane exhibited the lowest SSA but had the most favorable aerodynamic properties from the Handihaler® DPI compared to all other nanostructured amorphous solid dispersions produced by TFF in this study.

4. Discussion

4.1. Thin film freezing of VRC without excipients

Thin film freezing is an ultra rapid freezing process where a solution droplet freezes into thin films on a cryogenic surface within 50–1000 ms, depending on the properties of the solvent (Overhoff et al., 2007). The degree of supercooling of dilute solutions is so high that nucleation and growth of crystals may be minimized or prevented, leading to formation of amorphous material with nanostructure (Overhoff et al., 2009). However, without the inclusion of an adequate amount of high glass transition temperature stabilizing excipient, recrystallization of VRC will occur during the lyophilization process since the glass transition temperature of pure amorphous VRC was found to be about 1 °C. As predicted, thin film freezing of voriconazole solution without stabilizing excipients exhibited crystalline morphology (Figs. 5a and 6f). Interestingly, nanostructure was not maintained during lyophilization of TFF–VRC as the size of the primary particles grew during recrystallization.

4.2. Preformulation studies and evidence of formation of amorphous solid dispersion with PVP

PVP and HPMC are polymers with high glass transition temperatures, often used as crystallization inhibitors in the production of amorphous solid dispersions by the solvent method (Leuner and Dressman, 2000). In order to take advantage of the higher

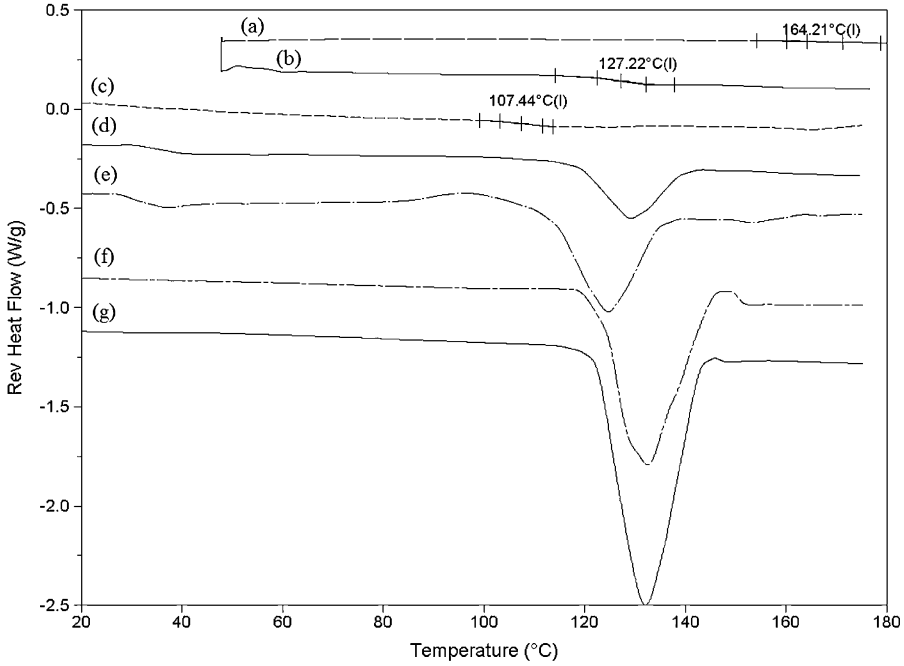

Fig. 6. Modulated DSC curves. (a) PVP K30; (b) PVP K12; (c) TFF–VRC–PVP K30 (1:2); (d) TFF–VRC–LAC–PVP K30 (1:1:1); (e) TFF–VRC–LAC (1:2); (f) TFF–VRC; and (g) crystalline VRC (as received from supplier).

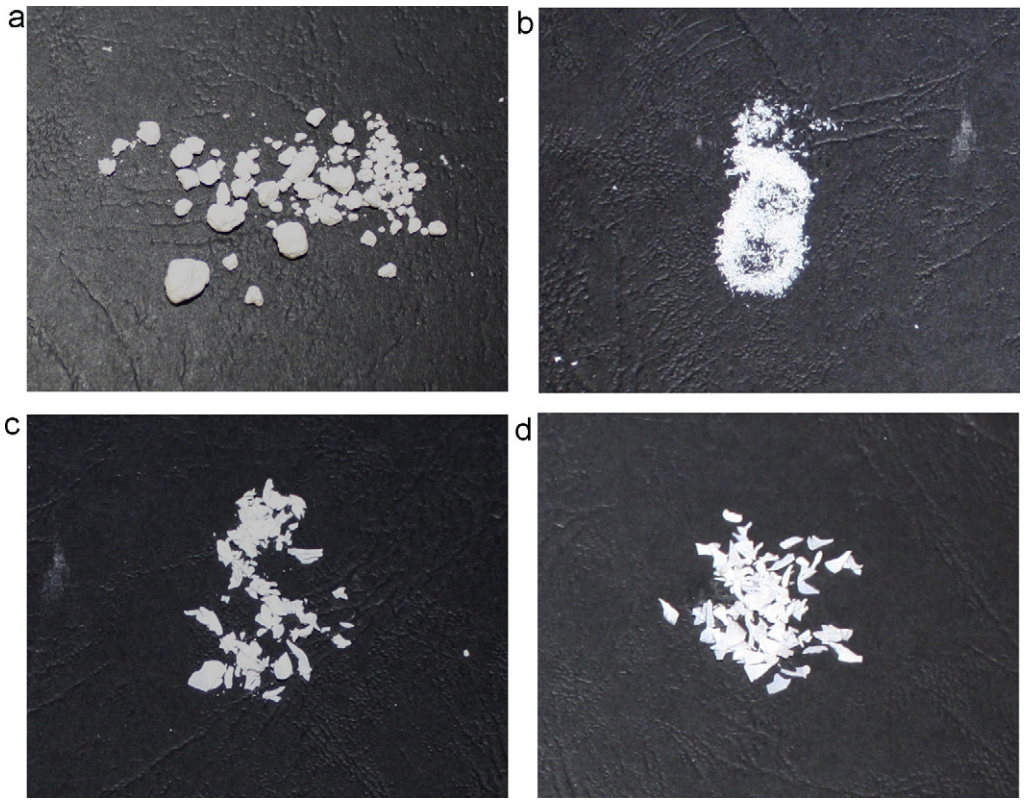

Fig. 7. Photos of the macroscopic appearance of TFF-processed powders containing VRC. (a) TFF formulations prepared using 1% (w/v) in 1,4-dioxane; (b) TFF formulations prepared using 0.1% (w/v) or 1% (w/v) in 50:50 1,4-dioxane:water; (c) TFF formulations prepared using 1% (w/v) in 20:80 1,4-dioxane:water; and (d) TFF formulations prepared using 10% (w/v) in 1,4-dioxane or 50:50 1,4-dioxane:water.

energy state and increased solubility of amorphous solids, the drug must remain in the amorphous state over pharmaceutically relevant time scales, typically at least 2 years. Two of the properties that are of particular importance with respect to physical stability of amorphous solid dispersions (or amorphous solid solutions) are the drug–polymer miscibility and the solubility of the crystalline drug in the polymer. Without drug–polymer miscibility, the solid dispersion may exist as two phases and the properties of the pure amorphous drug will primarily dominate the crystallization behavior of the pharmaceutical system. Thermal analysis of

Table 2
BET surface area measurements and bulk densities of TFF formulations containing VRC.

Sample composition	Dissolved solids	Solvent composition	SSA (m^2/g) Mean ± std. dev.	Average bulk density (g/cm^3)
TFF–VRC	0.1% (w/v)	50:50 (v/v) 1,4-Dioxane:water	9.4	–
	1% (w/v)	50:50 (v/v) 1,4-Dioxane:water	9.4 ± 3.2	0.058
		1,4-Dioxane	10.4	0.034
	10% (w/v)	1,4-Dioxane	5.3	0.075
TFF–VRC–PVP K12 (1:2)	1% (w/v)	1,4-Dioxane	23.4 ± 9.6	0.015
		50:50 (v/v) 1,4-Dioxane:water	83.7 ± 21.0	0.021
		20:80 (v/v) 1,4-Dioxane:water	73.5 ± 3.4	0.014
TFF–VRC–PVP K30 (1:2)	0.1% (w/v)	50:50 (v/v) 1,4-Dioxane:water	2.8 ± 1.7	–
		1,4-Dioxane	69.3 ± 5.3	0.018
	1% (w/v)	50:50 (v/v) 1,4-Dioxane:water	107.8 ± 12.4	0.021
		20:80 (v/v) 1,4-Dioxane:water	81.3 ± 22.3	0.014
	10% (w/v)	50:50 (v/v) 1,4-Dioxane:water	156.6 ± 13.7	0.070
TFF–VRC–PVP K30 (1:3)	1% (w/v)	50:50 (v/v) 1,4-Dioxane:water	167.3 ± 17.5	0.021

Table 3
Aerodynamic properties of TFF formulations containing VRC.

Sample composition	Dissolved solids	Solvent composition	Aerodynamic properties			
			EF (%)	FPF (%)	MMAD (μm)	GSD (μm)
TFF–VRC	0.1% (w/v)	50:50 (v/v) 1,4-Dioxane:water	89.4	28.6	5.1	2.5
	1% (w/v)	50:50 (v/v) 1,4-Dioxane:water	81.2	37.8	4.2	2.4
		1,4-Dioxane	80.6	43.1	3.5	2.2
	10% (w/v)	1,4-Dioxane	73.3	30.7	4.5	2.6
TFF–VRC–PVP K12 (1:2)	1% (w/v)	1,4-Dioxane	96.5	42.4	4.5	3.3
		50:50 (v/v) 1,4-Dioxane:water	83.3	20.0	>6	–
		20:80 (v/v) 1,4-Dioxane:water	91.4	26.8	>6	–
TFF–VRC–PVP K30 (1:2)	1% (w/v)	1,4-Dioxane	96.9	21.1	>6	–
		50:50 (v/v) 1,4-Dioxane:water	96.5	20.2	>6	–
		20:80 (v/v) 1,4-Dioxane:water	95.9	22.7	>6	–
	10% (w/v)	50:50 (v/v) 1,4-Dioxane:water	47.8	4.8	>6	–
TFF–VRC–PVP K30 (1:3)	1% (w/v)	50:50 (v/v) 1,4-Dioxane:water	96.6	28.4	>6	–

physical mixtures using DSC can be used to estimate drug–polymer miscibility by melting point depression (Marsac et al., 2009). A slight melting point depression indicates PVP may be a suitable biopolymer to inhibit crystallization of VRC from the amorphous state. Furthermore, the decrease in percent recovery of crystalline VRC as the amount of drug in the physical mixtures is decreased may be a sign that VRC partially dissolves into PVP upon heating (Dinunzio et al., 2010). On the other hand, preformulation studies revealed that HPMC would probably not be as suitable to form a stable amorphous solid dispersion with VRC as compared to PVP.

Drug–polymer miscibility and formation of a single phase amorphous solid solution, where drug and polymer are mixed at a molecular level, can also be assessed by modulated DSC. Observation of a single glass transition temperature at an intermediate temperature between the glass transitions of the individual components is evidence of a miscible system; whereas, observation of two glass transition temperatures is evidence of a two-phase system (Huang and Wigent, 2009). The Gordon–Taylor equation (Gordon and Taylor, 1952), presented in Equation 1, coupled with the Simha–Boyer rule (Simha and Boyer, 1962), presented as Eq. (2), may be used to predict T_{g12}, the glass transition temperature of the drug–polymer blend. w_1, w_2, T_{g1}, and T_{g2} are the weight fractions and glass transition temperatures (in K) of the drug and polymer, respectively, and ρ_1 and ρ_2 are the true densities of the drug and polymer.

$$T_{g12} = \frac{w_1 T_{g1} + K w_2 T_{g2}}{w_1 + K w_2} \quad (1)$$

$$K \cong \frac{\rho_1 T_{g1}}{\rho_2 T_{g2}} \quad (2)$$

The observed glass transition temperature of TFF–VRC–PVP K30 (1:2) is shown in Fig. 6c. A single glass transition temperature, similar to the predicted value using the Gordon–Taylor equation coupled with the Simha–Boyer rule, indicates that the amorphous pharmaceutical system exists as a single phase.

As demonstrated in the preformulation study, VRC may partially solubilize in PVP upon heating. Thus, powder XRD was conducted to assess the degree of crystallinity of the VRC–PVP solid dispersions produced by TFF since modulated DSC would not be able to detect the presence of low levels of crystalline material.

4.3. Effect of PVP grade on morphology and aerodynamic properties of TFF formulations

The TFF–VRC–PVP (1:2) formulations prepared from 1% (w/v) dissolved solids content in the various solvent systems were used to compare the effect of PVP grade on the SSA, bulk density, and aerodynamic performance of the amorphous solid dispersions produced by TFF. Specific surface area was significantly higher when PVP K30, a higher molecular weight grade of PVP, was used in the composition ($p = 0.0225$). Higher molecular weight polymers have increased strength and viscoelasticity. These properties will help PVP K30 more effectively stabilize the nanostructured matrix. On the other hand, the strength of the bridges between primary particles will negatively affect aerodynamic properties. Higher grades of PVP will create stronger bridges, which are more difficult to shear in situ, resulting in less respirable particles and significantly lower FPF ($p = 0.05$). PVP grade did not significantly impact bulk density.

4.4. Effect of solvent composition on morphology and aerodynamic properties of TFF formulations

The solvent system composition, specifically the aqueous content, affected the SSA of the TFF–VRC–PVP (1:2) formulations produced. The formulations manufactured with 100% 1,4-dioxane exhibit significantly lower SSA compared to their miscible aqueous-organic cosolvent counterparts ($p = 0.007$ for PVP K12 group; $p = 0.0286$ for PVP K30 group). The increase in SSA of the formulations prepared from miscible aqueous-organic cosolvent systems can be explained by the difference in solvent properties and droplet spreading of the solution upon impingement with the cryogenic surface. Even though the thin film geometry was not physically measured, it was visually apparent that the diameter of the thin films comprising 100% 1,4-dioxane were much smaller (approximately 1 cm) than the diameter of the thin films composed of 1,4-dioxane:water cosolvent mixtures (approximately 1.6 cm). A lower degree of spreading in the radial direction can be attributed to the higher viscosity of 1,4-dioxane compared to water (Mao et al., 1997). Furthermore, the solutions were dropped from the same height above the cryogenic surface with the same dispensing burette in all experiments, but due to higher surface tension

of the water compared to 1,4-dioxane (Wohlfarth, 2008), droplet volumes were different for each solvent system. Droplet volumes were determined by dropping 100 droplets into a graduated cylinder and measuring the total volume. The estimated droplet volumes for 1,4-dioxane, 50:50 (v/v) 1,4-dioxane:water, and 20:80 (v/v) 1,4-dioxane:water were 0.25, 0.33 and 0.40 mL, respectively. Using the volume (V) of one drop and the estimated diameter of the thin film, the thickness (h) of the films can be calculated and the surface area to volume ratio of the thin film can be approximated. For instance, for 1,4-dioxane drops, $h = V/(\pi \cdot r^2) = 0.0318$ cm. Therefore, surface area of the thin film is $SA = 2\pi \cdot r^2 + 2\pi \cdot r \cdot h = 1.67\ cm^2$ and the surface area to volume ratio is 67. Likewise, the thickness of a thin film made from 50:50 (v/v) 1,4-dioxane:water is 0.0164 cm and the surface area to volume ratio is 124; and the thickness of a thin film made from 20:80 (v/v) 1,4-dioxane:water is 0.0199 cm and the surface area to volume ratio is 103. Since the concentrations of the liquid feed solutions were the same (1%, w/v), smaller surface area to volume ratios will result in aggregate particles with lower specific surface area. Additionally, the film thickness, h, can be used to explain why the 20:80 (v/v) 1,4-dioxane:water films remained intact as thin flakes during lyophilization compared to 50:50 (v/v) 1,4-dioxane:water films. There was more particle bridging in the h-direction which made the flakes slightly more rigid, preventing breakage into fine, fluffy powders.

The degree of crystallinity of TFF–VRC–PVP (1:2) solid dispersions was observed to be directly proportional to the aqueous content used in the liquid feed solution (Fig. 5b–g). An explanation by two phenomena is proposed. First, water has a lower vapor pressure than 1,4-dioxane; and therefore, is more difficult to remove during lyophilization, especially the amount of bound water during secondary drying. Since water acts as a plasticizer in solid dispersions and will decrease the T_g and physical stability of the amorphous composition (Hancock and Zografi, 1994), it is likely the formulations manufactured using aqueous-organic cosolvent systems had higher residual water content leading to some recrystallization of the amorphous VRC. Second, VRC, PVP, and amorphous materials are hygroscopic. With the increased surface area available for moisture uptake (Telko and Hickey, 2005), there is a greater potential for recrystallization in amorphous solid dispersions with very high surface areas.

For the TFF–VRC formulations which resulted in crystal growth during lyophilization, the solvent system composition did not affect the SSA since the nanostructure could not be maintained without a polymeric stabilizer. However, the same observations were made during the TFF process: better droplet spreading with the aqueous-organic cosolvent system. Still, the solvent system composition exhibited the same effect on the macroscopic powder appearance for both crystalline and amorphous formulations. The cause for significant agglomeration of the TFF-processed powders produced with 100% 1,4-dioxane is not apparent.

When comparing the effect of solvent system composition on the aerodynamic performance of the TFF-processed powders, there is a trend that the macroscopic/bulk properties influence the FPF, with formulations prepared from 100% 1,4-dioxane performing the best, but the differences were not significant for either the crystalline group or the amorphous group. Therefore, the data indicates that SSA has the greatest influence on the fine particle fraction delivered to the lungs from low density, aggregate particles sheared in situ from the Handihaler® DPI.

4.5. Effect of dissolved solids content in liquid feed solution on morphology and aerodynamic properties of TFF formulations

For the crystalline TFF–VRC formulations, the dissolved solids content within the voriconazole solution was found to affect the primary particle structure of the aggregate particles. Brownian motion of particles can be used to explain interactions between drug molecules in solution (Mazo, 2002). At very dilute concentrations, the distance between molecules in the thin frozen films is so large that adequate bridging of particles could not occur during lyophilization, resulting in irregular crystal growth and non-homogeneity of the primary particle size (Fig. 3c). In concentrated solutions, particle collisions in solution are much more likely and the molecules are closer together. Therefore, when frozen, there are many more bridges occurring between molecules, and consequently, the void space appears to be reduced once the solvent is removed (Fig. 3d). At 1% (w/v) dissolved solids content, the primary particles are more homogeneous (Fig. 3e and f). It also looked like the dissolved solids content influenced the aerodynamic properties of the crystalline formulations. Higher dissolved solids content (10%, w/v) in the TFF feed solution led to a greater number of particle bridges within the low density, aggregate particles, which during aerosolization, were more difficult to shear resulting in a slightly lower emitted fraction (73.3% versus 80.6%) and FPF (30.7% versus 43.1%) and a slightly higher MMAD (4.5 μm versus 3.5 μm).

The formulations manufactured with VRC–PVP K30 (1:2) using 50:50 (v/v) 1,4-dioxane:water were used to compare the effect of dissolved solids content in the liquid feed solution on the surface area of the solid dispersion formulations. Surprisingly, the lowest dissolved solids content (0.1%, w/v) resulted in the lowest SSA and the highest dissolved solids content (10%, w/v) resulted in the highest SSA. All pairs were significantly different (2.8 m^2/g versus 107.8 m^2/g versus 156.6 m^2/g, $p = 0.0007$). In this case, VRC and PVP can interact more intimately within more concentrated solutions, due to Brownian motion of molecules, creating better stabilization of the amorphous VRC and the nanostructure during lyophilization. In very dilute solutions (0.1%, w/v), there was insufficient interaction between VRC and PVP leading to considerable recrystallization of VRC (Fig. 5h) and collapse of the nanostructure. On the other hand, 10% (w/v) dissolved solids content was found to significantly decrease the emitted fraction ($p = 0.0008$) from the Handihaler® DPI compared to 1% (w/v) dissolved solids content. It appeared that there was an increased number of particle bridges adding strength and elasticity that decreased the brittleness and prevented adequate shearing of the aggregate particles.

4.6. Effect of VRC to PVP ratio in amorphous solid dispersions

TFF–VRC–PVP K30 (1:2) and TFF–VRC–PVP K30 (1:3) produced from 1% (w/v) dissolved solids in 50:50 (v/v) 1,4-dioxane:water were used to compare the effect of drug to excipient ratio on morphology of the resulting formulations. The higher polymer level in the formulation composition was more effective at stabilizing VRC in the amorphous state, as indicated by XRD. From the Gordon–Taylor equation (Gordon and Taylor, 1952), a higher fraction of polymer in the solid dispersion will result in a higher glass transition. It is well known that a higher glass transition temperature will increase physical stability of the formulation (Hancock and Zografi, 1997). In fact, using a 1 to 3 drug to polymer ratio eliminated the adverse effect seen from the inclusion of water in the solvent system. Even with plasticization of the solid dispersion by water (Hancock and Zografi, 1994), 1 to 3 VRC to PVP ratio was able to form a physically stable solid dispersion at room temperature. Furthermore, SSA was significantly higher with lower drug loading (167.3 versus 107.8 m^2/g, $p = 0.0016$). Increased polymer content will not only stabilize amorphous VRC more effectively, it will also increase the strength of the drug–polymer matrix. Therefore, the nanostructure of the aggregate particles is preserved more effectively during lyophilization.

5. Conclusions

Engineered particles with enhanced powder properties containing voriconazole were successfully produced by the TFF process. Thin film freezing of voriconazole without stabilizing excipients exhibited crystalline morphology and the TFF process parameters, including solvent system composition and percentage of dissolved solids in the liquid feed solution, did not significantly influence the solid states properties and aerodynamic performance of the microstructured, crystalline aggregate particles. On the contrary, polymeric stabilization at a drug to excipient ratio of at least 1 to 2 was required to produce nanostructured, amorphous solid dispersions by the TFF process. All of the process parameters investigated, type/grade of stabilizing excipient, drug to excipient ratio, solvent system composition, and percentage of dissolved solids content in the liquid feed solution, significantly influenced the morphology and physicochemical properties of the resulting formulations. In summary, formulation of voriconazole by TFF with or without PVP resulted in low density, brittle matrix particles that could be sheared in situ into respirable particles from a passive inhalation dry powder inhaler. The solvent system composition in the TFF liquid feed solution affected droplet spreading upon impingement with the cryogenic surface; and therefore, determined the specific surface area and macroscopic powder appearance of the TFF-processed powders. It was these two solid state properties that were the most important factors influencing the aerodynamic properties of TFF-processed powders containing voriconazole.

Acknowledgments

The authors kindly acknowledge the financial support from Enavail LLC. NAB would also like to express her appreciation for the financial support provided by American Foundation for Pharmaceutical Education (AFPE) through the Pre-Doctoral Fellowship in Pharmaceutical Sciences from 2010 to 2011.

References

Bhavna Ahmad, F.J., Mittal, G., Jain, G.K., Malhotra, G., Khar, R.K., Bhatnagar, A., 2009. Nano-salbutamol dry powder inhalation: a new approach for treating broncho-constrictive conditions. Eur. J. Pharm. Biopharm. 71, 282–291.

Buchanan, C.M., Buchanan, N.L., Edgar, K.J., Ramsey, M.G., 2007. Solubilty and dissolution studies of antifungal drug:hydroxybutenyl-β-cyclodextrin complexes. Cellulose 14, 35–47.

Chow, A.H., Tong, H.H., Chattopadhyay, P., Shekunov, B.Y., 2007. Particle engineering for pulmonary drug delivery. Pharm. Res. 24, 411–437.

Dinunzio, J.C., Brough, C., Hughey, J.R., Miller, D.A., Williams 3rd., R.O., McGinity, J.W., 2010. Fusion production of solid dispersions containing a heat-sensitive active ingredient by hot melt extrusion and kinetisol dispersing. Eur. J. Pharm. Biopharm. 74, 340–351.

Doffman, S.R., Agrawal, S.G., Brown, J.S., 2005. Invasive pulmonary aspergillosis. Expert Rev. Anti Infect. Ther. 3, 613–627.

Edwards, D.A., Hanes, J., Caponetti, G., Hrkach, J., BenJebria, A., Eskew, M.L., Mintzes, J., Deaver, D., Lotan, N., Langer, R., 1997. Large porous particles for pulmonary drug delivery. Science 276, 1868–1871.

FDA, 2000. Guidance for Industry: Waiver of In Vivo Bioavailability and Bioequivalence Studies for Immediate-Release Solid Oral Dosage Forms Based on a Biopharmaceutics Classification System.

FisherScientific, 2009. Material Safety Data Sheet: 1,4-Dioxane.

Forster, A., Hempenstall, J., Tucker, I., Rades, T., 2001. Selection of excipients for melt extrusion with two poorly water-soluble drugs by solubility parameter calculation and thermal analysis. Int. J. Pharm. 226, 147–161.

Gabbott, P., Clarke, P., Mann, T., Royall, P., Shergill, S., 2003. A high-sensitivity, high-speed DSC technique: measurement of amorphous lactose. Am. Lab. 17.

Gordon, M., Taylor, J.S., 1952. Ideal copolymers and the second order transitions of synthetic rubbers. I. Non crystalline copolymers. J. Appl. Chem. 2, 493–500.

Hancock, B.C., Zografi, G., 1994. The relationship between the glass transition temperature and the water content of amorphous pharmaceutical solids. Pharm. Res. 11, 471–477.

Hancock, B.C., Zografi, G., 1997. Characteristics and significance of the amorphous state in pharmaceutical systems. J. Pharm. Sci. 86, 1–12.

Herbrecht, R., 2004. Voriconazole: therapeutic review of a new azole antifungal. Expert Rev. Anti Infect. Ther. 2, 485–497.

Huang, J., Wigent, R.J., 2009. Determination of drug and polymer miscibility and solid solubility for design of stable amorphous solid dispersions. Am. Pharm. Rev. (July/August), 18, 20,22,24–26.

Johnston, K.P., Engstrom, J., Tam, J., Watts, A., 2010. Compositions and Methods of Making Brittle-matrix Particles through Blister Pack Freezing. United States Patent & Trademark Office, US 2010/0221343.

Leuner, C., Dressman, J., 2000. Improving drug solubility for oral delivery using solid dispersions. Eur. J. Pharm. Biopharm. 50, 47–60.

Lipinski, C.A., 2000. Drug-like properties and the causes of poor solubility and poor permeability. J. Pharmacol. Toxicol. Methods 44, 235–249.

Mao, T., Kuhn, D.C.S., Tran, H., 1997. Spread and Rebound of Liquid Droplets upon Impact on Flat Surfaces. AIChE J. 43, 2169–2179.

Marsac, P.J., Li, T., Taylor, L.S., 2009. Estimation of drug–polymer miscibility and solubility in amorphous solid dispersions using experimentally determined interaction parameters. Pharm. Res. 26, 139–151.

Mazo, R.M., 2002. Brownian Motion: Fluctuations, Dynamics, and Applications. Oxford University Press, New York.

Mitchell, J.P., 2003. Practices of Coating Collection Surfaces of Cascade Impactors: A Survey of Members of the European Pharmaceutical Aerosol Group (EPAG), Drug Delivery to the Lungs-14. The Aerosol Society, London, UK, pp. 75–78.

Overhoff, K.A., Engstrom, J.D., Chen, B., Scherzer, B.D., Milner, T.E., Johnston, K.P., Williams 3rd., R.O., 2007. Novel ultra-rapid freezing particle engineering process for enhancement of dissolution rates of poorly water-soluble drugs. Eur. J. Pharm. Biopharm. 65, 57–67.

Overhoff, K.A., Johnston, K.P., Tam, J., Engstrom, J.D., Williams 3rd., R.O., 2009. Use of thin film freezing to enable drug delivery: a review. J. Drug Deliv. Sci. Technol. 19, 89–98.

Pascual, A., Nieth, V., Calandra, T., Bille, J., Bolay, S., Decosterd, L.A., Buclin, T., Majcherczyk, P.A., Sanglard, D., Marchetti, O., 2007. Variability of voriconazole plasma levels measured by new high-performance liquid chromatography and bioassay methods. Antimicrob. Agents Chemother. 51, 137–143.

Pfizer, 2011. VFEND® Prescribing Information [cited August 7, 2011]. Available from: http://www.pfizer.com/files/products/uspi_vfend.pdf.

Roffey, S.J., Cole, S., Comby, P., Gibson, D., Jezequel, S.G., Nedderman, A.N.R., Smith, D.A., Walker, D.K., Wood, N., 2003. The disposition of voriconazole in mouse, rat, rabbit, guinea pig, dog, and human. Drug Metab. Dispos. 31, 731–741.

Simha, R., Boyer, R., 1962. On a general relation involving the glass temperature and coefficients of expansion of polymers. J. Chem. Phys. 37, 1003.

Sinha, B., Mukherjee, B., 2012. Development of an inhalation chamber and a dry powder inhaler device for administration of pulmonary medication in animal model. Drug Dev. Ind. Pharm. 38, 171–179.

Sundaram, V., Uppala, V.B.R., Akundi, S.P., Muvva, V., Chitta, V., Donthula, A., Kharkar, M.R., Devarakonda, S.N., Peddireddy, S.R., 2008. Process for Preparing Voriconazole. United States Patent & Trademark Office, US 2008/0194820.

Telko, M.J., Hickey, A.J., 2005. Dry powder inhaler formulation. Respir. Care 50, 1209–1227.

United States Pharmacopeia (USP), 2010a. General Chapter 601: Aerosols, Nasal Sprays, Metered-dose Inhalers, and Dry Powder Inhalers. USP 32-NF 27, Rockville, MD, USA.

United States Pharmacopeia (USP), 2010b. General Chapter 647: Residual Solvents. USP 32-NF 27, Rockville, MD, USA.

Wohlfarth, C., 2008. Surface Tension of Pure Liquids and Binary Liquid Mixtures (Supplement to IV/16). Springer, Berlin.

Xie, Y., Zeng, P., Wiedmann, T.S., 2008. Disease guided optimization of the respiratory delivery of microparticulate formulations. Expert Opin. Drug Deliv. 5, 269–289.

Yang, W., Peters, J.I., Williams, R.O., 2008a. Inhaled nanoparticles – a current review. Int. J. Pharm. 356, 239–247.

Yang, W., Tam, J., Miller, D.A., Zhou, J., McConville, J.T., Johnston, K.P., Williams, R.O., 2008b. High bioavailability from nebulized itraconazole nanoparticle dispersions with biocompatible stabilizers. Int. J. Pharm. 361, 177–188.

Zhang, J., Wu, L., Chan, H.K., Watanabe, W., 2011. Formation, characterization, and fate of inhaled drug nanoparticles. Adv. Drug Deliv. Rev. 63, 441–455.